Inorganic Chemistry

Article

pubs.acs.org/IC

Solvent-Induced Controllable Synthesis, Single-Crystal to Single-Crystal Transformation and Encapsulation of Alq3 for Modulated Luminescence in (4,8)-Connected Metal–Organic Frameworks

Ya-Qian Lan,[†,‡,§] Hai-Long Jiang,[†,§] Shun-Li Li,[‡] and Qiang Xu*[,†]

[†]National Institute of Advanced Industrial Science and Technology (AIST), Ikeda, Osaka 563-8577, Japan

[‡]Faculty of Chemistry, Northeast Normal University, Changchun 130024, P. R. China

Supporting Information

ABSTRACT: In this work, for the first time, we have systematically demonstrated that solvent plays crucial roles in both controllable synthesis of metal–organic frameworks (MOFs) and their structural transformation process. With solvent as the only variable, five new MOFs with different structures have been constructed, in which one MOF undergoes solvent-induced single-crystal to single-crystal (SCSC) transformation that involves not only solvent exchange but also the cleavage and formation of coordination bonds. Particularly, a significant crystallographic change has been realized through an unprecedented three-step SCSC transformation process. Furthermore, we have demonstrated that the obtained MOF could be an excellent host for chromophores such as Alq3 for modulated luminescent properties.

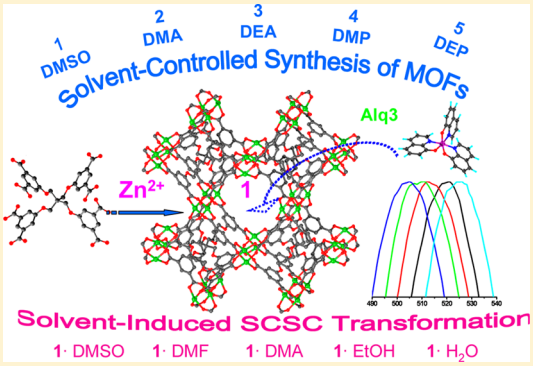

INTRODUCTION

Metal–organic frameworks (MOFs) have been focus of great interest due to not only their structural and chemical diversity but also structure-related potential applications, such as luminescence, sorption and separation, catalysis, etc.[1−3] The modular nature of MOFs make them highly tunable and the main strategy to construct of MOFs with diversified molecular architectures is currently based on judicious choices of metal (cluster) centers and predesigned ligand with specific geometry.[1a,3] In contrast, less attention have been received on the influences of experimental synthesis parameters, of which solvent plays a significant role in the determination of activation energetics and reaction thermodynamics, and thus the resultant MOF structures.[4] On the other hand, structural changes between MOFs triggered by external stimulus, such as, light, heat, and solvent, etc., are particularly intriguing.[5] Although structural transformation demonstrated by powder-phase is familiar, single-crystal to single-crystal (SCSC) transformation is much less because MOFs hardly retain the single crystallinity upon transformation.[6,7] Moreover, guest molecule exchange is involved in most of the reported cases of SCSC transformation. It is rare that coordination bond cleavage and formation happen to the coordination spheres of metal centers during the transformation process,[7] where MOFs are usually accompanied by loss of crystallinity, thus preventing the identification of the products. It is of particular importance to understand the role of solvent in the structure formation/evolvement and there have been a few reports on MOF structures affected by solvent effect.[7] However, systematic studies on different solvents for MOF formation and structural transformation still remain scarce.

Recently, luminescent functional MOFs have been reviewed by Qian and Chen.[8] Certainly, MOFs can be very promising as multifunctional luminescent materials,[9] because both the inorganic and the organic moieties can provide the platforms to generate luminescence, while metal–ligand charge transfer related to luminescence within MOFs can add other dimensional luminescent functionalities. Furthermore, the highly regular channel structures and controllable pore sizes of MOFs permit their applications in some guest molecule adsorption, which can also emit and/or induce luminescence. Since first developed as an efficient organic light emitting diode (OLED) in 1987, the Alq3 chromophore has attracted tremendous attention because of its wide range of applications in photoluminescence, electroluminescence, and field-emission.[10] Investigations have shown that the inclusion of chromophores into nanochannels or interlayer space can prevent their aggregation and improve the photochemical properties,[11] which motivates us to investigate the modulation of its luminescence by confining it in MOF pores.

Some microporous MOFs have been reported based on the semirigid octacarboxylic acid (5,5′-(2,2-bis((3,5-dicarboxyphenoxy) methyl)propane-1,3-diyl)bis(oxy)diisophthalic acid, H_8L) (Scheme 1) and transition metal cations (Zn^{II}, Cu^{II} and Cd^{II}) by Cao and Zhou groups recently.[12,13] In this work, with the same ligand H_8L and $Zn(NO_3)_2\bullet 6H_2O$ but different

Received: December 7, 2011
Published: June 26, 2012

 © 2012 American Chemical Society dx.doi.org/10.1021/ic202635a | Inorg. Chem. 2012, 51, 7484–7491

Scheme 1. Two-Step Synthesis Routes of H_8L

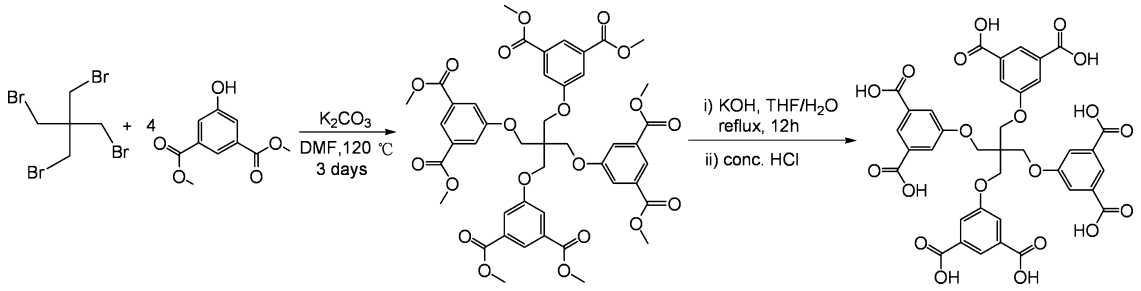

organic solvents as starting materials, we have controllably synthesized one (3,8)- and four (4,8)-connected microporous Zn-MOFs, one of which undergoes both isolated and coordinated solvent-substituted SCSC tranformations induced by solvent exchanges to afford four new MOFs. To the best of our knowledge, this is the first systematic study on various solvent-controlled roles on not only self-assembly but also SCSC transformation in MOFs. In addition, we have incorporated classical chromophore Alq3 into the MOF with appropriate pore size, highlighting the important example of Alq3-MOF hybrid with modulated luminescent emission and prolonged lifetime.

EXPERIMENTAL SECTION

Materials and Instrumentation. Chemicals were purchased from commercial sources and used without further purification. Powder X-ray diffraction (PXRD) was carried out with an X-ray diffractometer of Rigaku, Rint 2000. The FT-IR spectra were recorded from KBr pellets in the range 4000−400 cm^{-1} on a Mattson Alpha-Centauri spectrometer. The C, H, and N elemental analyses were conducted on a Perkin-Elmer 240C elemental analyzer. All samples were immersed in dichloromethane for 24 h. After the removal of dichloromethane by decanting, the sample was dried under a dynamic vacuum at room temperature overnight. ICP was measured by ICP-9000(N+M) (USA Thermo Jarrell-Ash Corp). ^1H NMR spectra were recorded at 25 °C on a Varian 500 MHz. Thermogravimetric analyses (TGA) were carried out on a Perkin-Elmer TG-7 analyzer heated from room temperature to 600 °C at a ramp rate of 5 °C/min under nitrogen. The photoluminescence (PL) spectra were measured on a Perkin-Elmer FLS-920 spectrometer. The N_2 sorption measurements were performed on automatic volumetric adsorption equipment (Belsorp mini II). Before gas adsorption measurements, the sample was immersed in dichloromethane for 24 h, and the extract was decanted. Fresh dichloromethane was subsequently added, and the crystals were allowed to stay for an additional 24 h to remove the nonvolatile solvates. Before the measurement, the sample was activated by drying under a dynamic vacuum at room temperature overnight and was dried again by using the 'outgas' function of the surface area analyzer for 12 h at room temperature.

Synthesis of H_8L. H_8L was synthesized according to the literature descriptions.[12,13]

The First Step. A mixture of pentaerythrityl tetrabromide (3.87 g, 10.0 mmol), dimethyl 5-hydroxyisophthalate (8.40 g, 40.0 mmol), and K_2CO_3 (16.58 g, 120 mmol) in *N*,*N*-dimethylformamide (DMF) (50 mL) was heated under vigorous stirring at 120 °C for 72 h. The reaction mixture was cooled to room temperature and then poured into 200 mL of water. A white solid of tetramethyl 5,5′-(2,2-bis((3,5-bis(methoxycarbonyl)phenoxy)methyl)propane-1,3-diyl)bis(oxy)-diiso-phthalate formed immediately, which was isolated by filtration in 95% yield after drying in vacuum.

The Second Step. In a round-bottom flask, tetramethyl 5,5′-(2,2-bis((3,5-bis(methoxycarbonyl)phenoxy)methyl)propane-1,3-diyl)bis-(oxy)diiso-phthalate (9.04 g, 10 mmol) was dissolved in tetrahydrofuran (THF) (150 mL) and a solution of KOH (11.22 g, 200 mmol) in H_2O (50 mL) was added. This mixture was refluxed for 12 h. After cooling down to room temperature, THF was evaporated and the resulting water phase was acidified with conc. HCl until no further precipitate was detected. The slightly white solid 5,5′-(2,2-bis((3,5-dicarboxyphenoxy)methyl)propane-1,3-diyl)bis(oxy)diisophthalic acid (H_8L) was collected by filtration, washed with water and dried in vacuum (7.13 g, 90%). ^1H NMR (DMSO-d_6, 500 MHz) δ: 4.47 (s, 8H), 7.69 (s, 8H), 8.03 (s, 4H), 13.27 (s, broad, 8H). IR (cm^{-1}): 3860 (w), 3741 (w), 3423 (s), 1695 (s), 1597 (s), 1462 (m), 1395 (s), 1215 (s), 1113 (m), 1041 (m), 903 (w), 761 (m), 729 (w), 665 (m).

Synthesis of Compound 1·DMSO. A solid mixture of H_8L (0.079 g, 0.1 mmol) and $Zn(NO_3)_2{\cdot}6H_2O$ (0.119 g, 0.4 mmol) was dissolved in a mixture of dimethyl sulfoxide (DMSO) and ethanol (5.0/5.0 mL) in a 20 mL Teflon-lined stainless steel container. The clear reaction solution was heated in an isotherm oven at 85 °C for 72 h, resulting in colorless block crystals of $Zn_4(L)(DMSO)_2(H_2O)_2{\cdot}xS$ (S = noncoordinated solvent molecules), which were washed with DMSO and collected. Yield: 0.100 g, 81% based on 1 mol of H_8L. Elemental microanalysis for desolvated **1**·DMSO ($Zn_4(L)(DMSO)_2(H_2O)_2$ = $C_{41}H_{36}O_{24}S_2Zn_4$), calculated (%): C, 39.76; H, 2.93. Found (%): C, 39.96; H, 3.01. IR (cm^{-1}): 3843 (w), 3742 (m), 3668 (w), 3440 (s), 2952 (m), 1643 (s), 1515 (s), 1454 (s), 1262 (m), 1106 (s), 1067 (m), 1023 (s), 952 (m), 778 (w), 719 (w), 550 (w), 453 (m).

Synthesis of Compound 1·DMF. *The First Method.* The same synthetic condition as that of **1**·DMSO was used except for DMF (5.0 mL) instead of DMSO/ethanol (5.0/5.0 mL). The colorless block crystals of $Zn_4(L)(DMF)_2(H_2O)_2{\cdot}xS$ (S = noncoordinated solvent molecules) were isolated by washing with DMF and collected. Yield: 0.076 g, 62% based on 1 mol of H_8L. Elemental microanalysis for desolvated **1**·DMF ($Zn_4(L)(DMF)_2(H_2O)_2$ = $C_{43}H_{38}N_2O_{24}Zn_4$), calculated (%): C, 42.04; H, 3.12; N, 2.28. Found (%): C, 42.06; H, 3.08; N, 2.30. IR (cm^{-1}): 3439 (s), 2941 (m), 1656 (s), 1516 (m), 1393 (s), 1261 (s), 1192 (w), 1104 (m), 944 (w), 884 (w), 787 (m), 716 (m), 594 (w), 469 (w).

The Second Method. Freshly prepared compound **1**·DMSO (0.100 g) was soaked in DMF solutions (10 mL) in a 20 mL Teflon-lined stainless steel container, which was heated in an isotherm oven at 85 °C for 72 h. The colorless block crystals of **1**·DMF were isolated by washing with DMF.

Synthesis of Compound 1·DMA. Freshly prepared compound **1**·DMSO (0.100 g) was soaked in *N*,*N*-dimethylacetamide (DMA) solutions (10 mL) in a 20 mL Teflon-lined stainless steel container, which was heated in an isotherm oven at 85 °C for 72 h. The colorless block crystals of $Zn_4(L)(DMA)_2(H_2O)_2{\cdot}xS$ (S = noncoordinated solvent molecules) were isolated by washing with DMA and collected. Elemental microanalysis for desolvated **1**·DMA ($Zn_4(L)(DMA)_2(H_2O)_2$ = $C_{45}H_{42}N_2O_{24}Zn_4$), calculated (%): C, 42.02; H, 3.37; N, 2.23. Found (%): C, 42.04; H, 3.39; N, 2.26. IR (cm^{-1}): 3442 (s), 2940 (m), 1628 (s), 1512 (m), 1454 (s), 1406 (s), 1261 (s), 1189 (w), 1124 (m), 1044 (m), 963 (w), 922 (w), 886 (w), 777 (m), 720 (m), 594 (w), 449 (w).

Synthesis of Compound 1·EtOH. The same synthetic procedure as that of **1**·DMA was used except for ethanol (10.0 mL) instead of DMA (10.0 mL). The colorless block crystals of $Zn_4(L)(EtOH)_2(H_2O)_2{\cdot}xS$ (S = noncoordinated solvent molecules) were

dx.doi.org/10.1021/ic202635a | *Inorg. Chem.* 2012, 51, 7484−7491

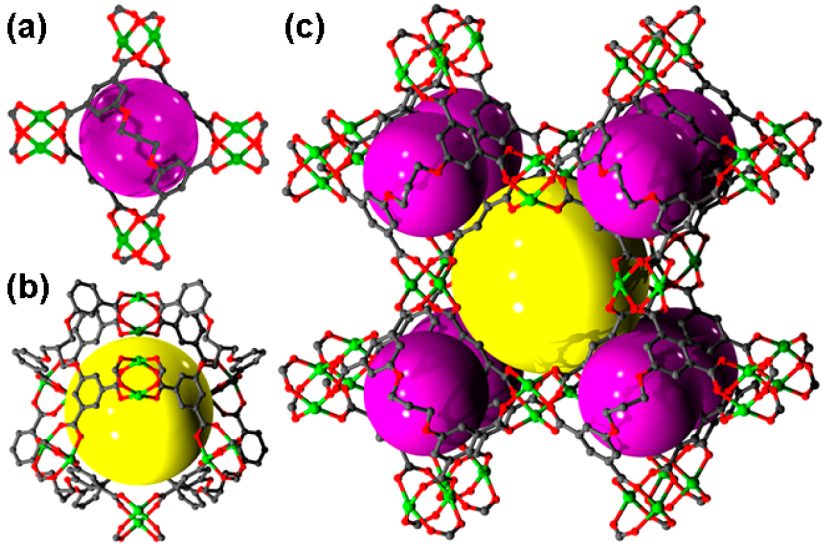

Figure 1. (a and b) Two types of cages in **1**·DMSO and (c) the structural feature of **1**·DMSO involving eight small cages and one large cage, highlighted with yellow and purple spheres that fit in the cavities without touching the frameworks. Carbon, gray; oxygen, red; zinc, green. All hydrogen atoms have been omitted for clarity.

isolated by washing with ethanol and collected. Elemental microanalysis for desolvated **1**·EtOH ($Zn_4(L)(EtOH)_2(H_2O)_2$ = $C_{41}H_{36}O_{24}Zn_4$), calculated (%): C, 41.93; H, 3.09. Found (%): C, 41.90; H, 3.05. IR (cm^{-1}): 3843 (w), 3741(w), 3419 (s), 2975 (m), 1617 (s), 1564 (s), 1454 (s), 1378 (s), 1266 (m), 1128 (m), 1045 (s), 881 (w), 777 (w), 725 (w), 595 (w), 452 (w).

Synthesis of Compound 1·H$_2$O. Freshly prepared compound **1**·EtOH was placed in a very slow stream of air for 12 h. The colorless block crystals of $Zn_4(L)(H_2O)_4$·*x*S (S = noncoordinated solvent molecules) were obtained. Elemental microanalysis for desolvated **1**·H_2O ($Zn_4(L)(H_2O)_4$ = $C_{37}H_{28}O_{24}Zn_4$), calculated (%): C, 39.74; H, 2.52. Found (%): C, 39.86; H, 2.57. IR (cm^{-1}): 3843 (w), 3741(w), 3442 (s), 2952 (m), 1643 (s), 1512 (m), 1454 (s), 1262 (m), 1109 (s), 1045 (m), 950 (m), 778 (w), 720 (w), 598 (w), 455 (w).

Synthesis of Compound 2. The same synthetic condition as that of **1**·DMSO was used except for DMA (5.0 mL) instead of DMSO/ethanol (5.0/5.0 mL). The colorless block crystals of $Zn_4(L)(DMA)(H_2O)_3$·*x*S (S = noncoordinated solvent molecules) were isolated by washing with DMA and collected. Yield: 0.089 g, 75% based on 1 mol of H_8L. Elemental microanalysis for desolvated **2** ($Zn_4(L)(DMA)(H_2O)_3$ = $C_{41}H_{35}NO_{24}Zn_4$), calculated (%): C, 42.04; H, 3.12; N, 2.28. Found (%): C, 42.07; H, 3.07; N, 2.24. IR (cm^{-1}): 3415 (s), 2940 (s), 1626 (s), 1507 (m), 1404 (s), 1262 (s), 1191 (w), 1105 (m), 1019 (m), 963 (w), 778 (w), 723 (w), 597 (m), 478 (w).

Synthesis of Compound 3. The same synthetic condition as that of **1**·DMSO was used except for N,N-diethylacetamide (DEA, 5.0 mL) instead of DMSO/ethanol (5.0/5.0 mL). The colorless block crystals of $Zn_9(L)_2(O)(DEA)_4(H_2O)_5$·*x*S (S = noncoordinated solvent molecules) were isolated by washing with DEA and collected. Yield: 0.076 g, 56% based on 1 mol of H_8L. Elemental microanalysis for desolvated **3** ($Zn_9(L)_2(O)(DEA)_4(H_2O)_5$ = $C_{98}H_{102}N_4O_{50}Zn_9$), calculated (%): C, 43.20; H, 3.77; N, 2.06. Found (%): C, 43.16; H, 3.67; N, 2.00. IR (cm^{-1}): 3425 (s), 2940 (s), 1625 (s), 1491 (m), 1401 (s), 1384 (s),1262 (s), 1161 (w), 1125 (m), 1049 (m), 963 (w), 778 (w), 720 (w), 597 (m), 475 (w).

Synthesis of Compound 4. The same synthetic condition as that of **1**·DMSO was used except for *N*,*N*-dimethylpropionamide (DMP, 5.0 mL) instead of DMSO/ethanol (5.0/5.0 mL). The colorless block crystals of $Zn_{10}(L)_2(O)_2(DMP)_2(H_2O)_9$·*x*S (S = noncoordinated solvent molecules) were isolated by washing with DMP and collected. Yield: 0.113 g, 86% based on 1 mol of H_8L. Elemental microanalysis for desolvated **4** ($Zn_{10}(L)_2(O)_2(DMP)_2(H_2O)_9$ = $C_{84}H_{80}N_2O_{53}Zn_{10}$), calculated (%): C, 38.51; H, 3.08; N, 1.07. Found (%): C, 38.66; H, 3.07; N, 1.00. IR (cm^{-1}): 3422 (s), 2940 (m), 1623 (s), 1457 (m), 1380 (s), 1267 (s), 1160 (w), 1130 (w), 1060 (m), 964 (w), 888 (w), 778 (m), 719 (m), 587 (w), 473 (w).

Synthesis of Compound 5. The same synthetic condition as that of **1**·DMSO was used except for N,N-diethylpropionamide (DEP, 5.0 mL) instead of DMSO/ethanol (5.0/5.0 mL). The colorless block crystals of $[Zn_{16}(L)_3(H_2O)_{16}](NO_3)_8$·*x*S (S = noncoordinated solvent molecules) were isolated by washing with DEP and collected. Yield: 0.114 g, 82% based on 1 mol of H_8L. Elemental microanalysis for desolvated **5** ($[Zn_{16}(L)_3(H_2O)_{16}](NO_3)_8$ = $C_{111}H_{92}N_8O_{100}Zn_{16}$), calculated (%): C, 31.86; H, 2.22; N, 2.68. Found (%): C, 31.96; H, 2.27; N, 2.80. IR (cm^{-1}): 3860 (w), 3741 (w), 3423 (s), 2941 (m), 1625 (s), 1462 (m), 1381 (s), 1250 (s), 1160 (w), 1061 (m), 964 (w), 778 (m), 719 (m), 587 (w), 477 (w).

Encapsulation of Alq3 in 1·DMSO. Different amounts of Alq3 was dissolved in DMF (10 mL) to afford 0.05, 0.10, 0.50, 1.0, 2.0, and 5.0 mmol/L Alq3 DMF solutions. Freshly prepared compounds **1**·DMSO were ground and soaked in DMF solutions of Alq3. After they were soaked for three days, the fluorescence spectra and lifetimes of these suspensions were examined.

X-ray Crystallography. Single-crystal X-ray data of all compounds were recorded by using a Bruker Apex CCD diffractometer with graphite-monochromated Mo Kα radiation (λ = 0.71073 Å) at T = 293 K. Absorption corrections were applied by using a multiscan technique. All the structures were solved by the direct method of SHELXS-97[14a] and refined by full-matrix least-squares techniques using the SHELXL-97 program[14b] within WINGX.[14c] Non-hydrogen atoms were refined with anisotropic temperature parameters. The H atoms of the ligand could not be introduced in the refinement but were included in the structure factor calculation. The solvent molecules are highly disordered, and attempts to locate and refine the solvent peaks were unsuccessful. Contributions to scattering due to these solvent molecules were removed using the SQUEEZE routine of PLATON,[14d] structures were then refined again using the data generated. Crystal data are summarized in Supporting Information Table S1.

■ RESULTS AND DISCUSSION

With solvent as the only variable, solvothermal reactions with the same amounts of $Zn(NO_3)_2·6H_2O$ and octacarboxylic acid ligand (H_8L) in DMSO/EtOH, DMA, DEA, DMP, and DEP, respectively, yielded $Zn_2(L)_{0.5}(DMSO)(H_2O)$ (**1**·DMSO), $Zn_4(L)(DMA)(H_2O)_3$ (**2**), $Zn_9(L)_2(O)(DEA)_4(H_2O)_5$ (**3**), $Zn_{10}(L)_2(O)_2(DMP)_2(H_2O)_9$ (**4**), and $[Zn_8(L)_{1.5}(H_2O)_8]$-

dx.doi.org/10.1021/ic202635a | *Inorg. Chem.* 2012, 51, 7484−7491

$(NO_3)_4$ (**5**) under the same reaction conditions. All the MOFs feature different structures based on single crystal X-ray structural analyses (Supporting Information Table S1).

The 3D framework of **1**·DMSO crystallizes in the space group of *Pbcm*. The asymmetric unit contains one L ligand, three Zn atoms, one DMSO and one H_2O, where L and two of Zn atoms have a half occupancy factor. There are two types of Zn_2 clusters, both of which are similarly coordinated by DMSO or H_2O molecules as axial groups, and four carboxylates from four bridging L ligands in a classical paddle-wheel mode, acting as a planar 4-connected node; the L connects to eight Zn_2 clusters. Such connectivity leads to a (4,8)-connected **scu** network with two types of cages (Figures 1 and 2 and Supporting Information Figure S1). Each large cage with size of 1.2 nm is surrounded by eight small cages of 0.8 nm, which contributes to the free porosity of 65.5%.[14d]

Compound **2** in $P4_32_12$ space group involves three H_2O, one L, and four Zn atoms that form two types of Zn_2 clusters in its asymmetric unit. Both clusters are coordinated by four carboxylate groups from four L ligands and either one DMA and one H_2O or two H_2O molecules as terminal groups, serving as tetrahedral nodes, and each L coordinates to eight Zn_2 clusters to be an 8-connected node, resulting in a 3D network

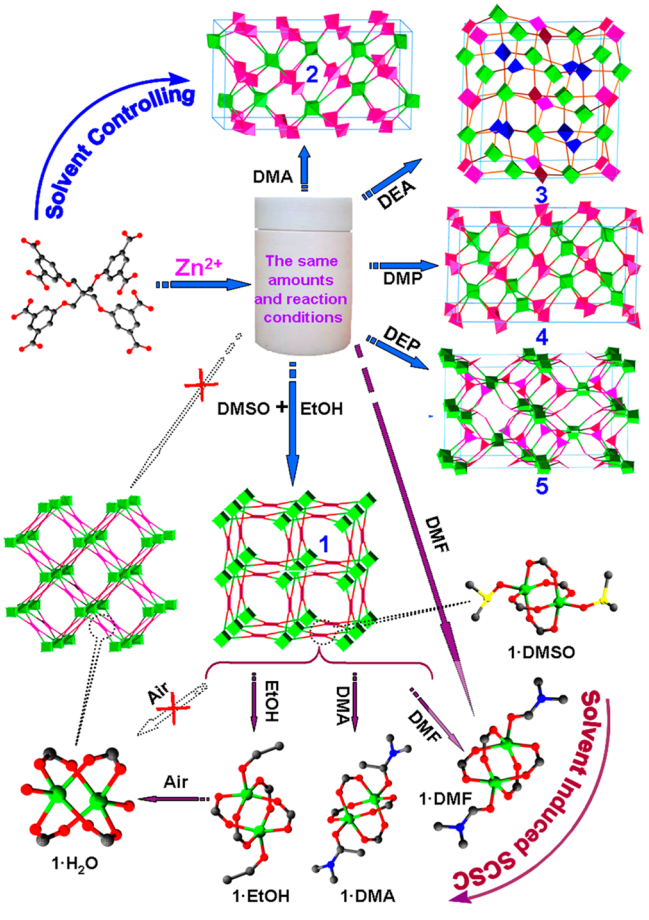

Figure 2. Schematic illustration for the solvent-controlled synthesis of compounds **1**–**5** (with blue arrows) and solvent-induced SCSC transformation/stepwise synthesis of other MOFs (with purple arrows) from **1**·DMSO. The topological structures are presented in the solvent-controlled synthesis part, and topological structure of **1**·H_2O and only coordination environments of Zn_2 clusters are displayed for the compounds in the SCSC transformation part.

with (4,8)-connected fluorite topology (Figure 2 and Supporting Information Figure S2).

There are two independent L ligands, one μ_3-O, nine Zn atoms, four DEA and five H_2O molecules in the asymmetric unit of **3** in $Pna2_1$ space group. The nine Zn atoms are interconnected by oxygen atoms to present three types of Zn_2 and one Zn_3 clusters. Two di-zinc(II) paddle-wheel clusters are similarly coordinated by one H_2O and one DEA molecules as axial ligands, and also four carboxylate groups from four L ligands to act as 4-connected nodes in a planar fashion. The other Zn_2 cluster is terminally coordinated by one H_2O and also coordinated by four carboxylate groups from four L ligands to be a tetrahedral node. The remaining Zn atoms share a μ_3-O to form Zn_3 cluster, which further grafted by one H_2O and two DEA molecules, and coordinated by four carboxylate groups from four L ligands, behaving as the other tetrahedral node. Both L ligands similarly coordinate to four planar and four tetrahedral Zn clusters (Supporting Information Figure S3). Such connectivity affords a complicated network that features a (4,8)-connected topology with Schläfli symbol of $(4^4{\cdot}6^2)_2(4^{16}{\cdot}6^{12}){\cdot}(4^{15}{\cdot}6^9{\cdot}8^4)$, calculated by OLEX[15] (Figure 2).

Compound **4** crystallizes in a chiral space group $P2_12_12_1$ and contains two L ligands, two μ_3-O, ten Zn atoms, two DMP and nine H_2O molecules in its asymmetric unit. The ten Zn atoms exist in the form of two Zn_2 and two Zn_3 clusters, all of which behave as tetrahedral nodes. Both Zn_2 clusters are coordinated by one H_2O and four carboxylate groups from four L ligands. Each of Zn_3 cluster has a sharing μ_3-O atom in their centers and was coordinated by four carboxylate groups from four L ligands and also terminally coordinated by either four H_2O or two DMP and two H_2O molecules. Both L ligands similarly coordinate to four types of Zn clusters as 8-connected nodes (Supporting Information Figure S4). The above complicate connection fashion of Zn clusters and L also leads to a 3D framework with (4,8)-connected fluorite topology (Figure 2), similar to that of **2**.

Compound **5** in $P\bar{4}n2$ space group has a more complicated structure (Figure 3 and Supporting Information Figure S5). It contains four L ligands, two of which have a half and the rest of which have a 1/4 occupancy factor, eight Zn atoms in the form of four Zn_2 clusters, eight coordinated H_2O molecules and four isolated NO_3^- ions for charge compensation in the asymmetric unit. Different from all Zn clusters described in previous cases, all the Zn_2 clusters in compound **5** have similar coordination modes by two H_2O as terminal groups and three carboxylate groups from three L ligands to behave as planar triangular nodes. All four L ligands are 8-connected, in which two L ligands connect to two types of Zn clusters, whereas the other two L ligands coordinate to all four types of Zn clusters (Supporting Information Figure S5). Accordingly, a (3,8)-connected topology with Schläfli symbol of $(4^3)(4^2{\cdot}6){\cdot}(4^8{\cdot}6^8{\cdot}8^{12}){\cdot}(4^8{\cdot}6^4{\cdot}8^{12}{\cdot}10^4)$ calculated by OLEX[15] that was never reported has been constructed (Figure 2). Offering further insight into the nature of this intricate architecture, the framework is comprised of five types of cage-like pore structures (Figure 3). PLATON[14d] analysis shows that the porosity is 68.9% in **5** after removed guest solvates.

Such vast diversity of Zn–L architectures controlled by solvent as the only variable is very amazing and rarely reported, which could be mainly ascribed to the flexible and mutidentate ligand. It is noteworthy that the obtained (4,8)-connected frameworks are also relatively rare compared to the classical topologies of diamond, NbO, and PtS etc.[16] So far, the limited

dx.doi.org/10.1021/ic202635a | *Inorg. Chem.* 2012, 51, 7484–7491

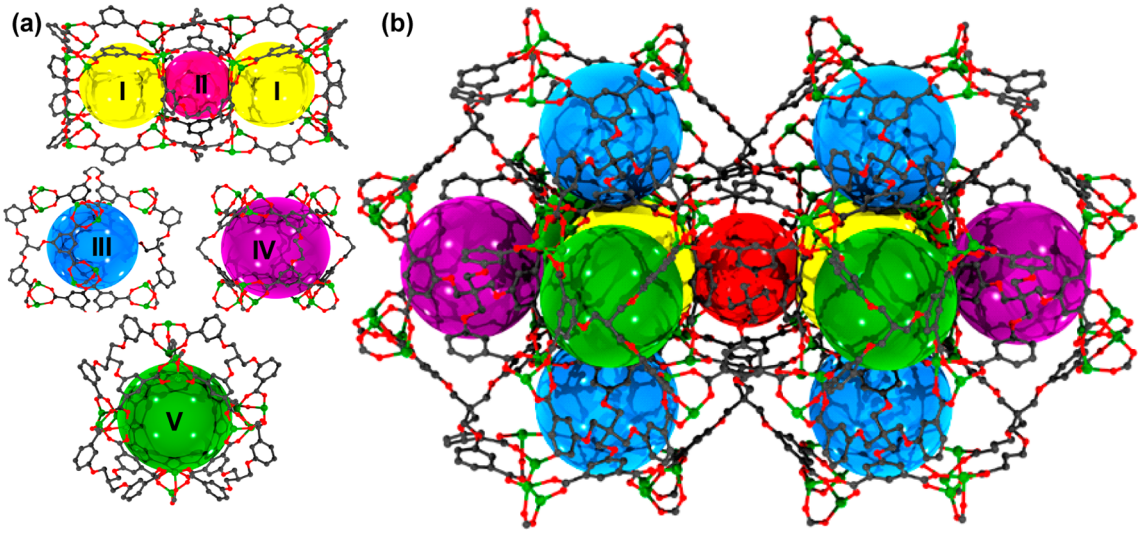

Figure 3. (a) Independent view of different types of cage structures. (b) Whole view of the complicated structure of **5** with different types of cages.

MOFs with (4,8)-connected topology mostly have a fluorite structure built from tetrahedral and cubical nodes and only a few MOFs with **scu** network involving square-planar and cubical nodes have been reported.[17,18] As far as we know, the (4,8)-connected topology, that compound **3** features, constructed from square-planar, tetrahedral and cubical nodes, has not been reported yet (Supporting Information Figure S6).

Five microporous Zn-MOFs (**1**·DMSO, **2**, **3**, **4**, and **5**) have been synthesized based on the ligand H_8L, $Zn(NO_3)_2{\cdot}6H_2O$ and different organic solvents (DMSO/EtOH, DMA, DEA, DMP, and DEP) under the same reaction conditions, respectively. Comparing these structures of MOFs, we find that different MOFs have been constructed from different types of Zn clusters. There are two types of Zn_2 clusters, which are coordinated by DMSO or H_2O molecules and four carboxylate groups in **1**·DMSO (Supporting Information Figure S1b). Two types of Zn_2 clusters are coordinated by four carboxylate groups and either one DMA and one H_2O or two H_2O molecules as terminal group in compound **2** (Supporting Information Figure S2b). There are three types of Zn_2 and one Zn_3 clusters in compound **3** (Supporting Information Figure S3b). Compound **4** contains two types of Zn_2 and two types of Zn_3 clusters (Supporting Information Figure S4b). All the Zn_2 clusters in compound **5** have similar coordination modes by two H_2O as terminal groups and three carboxylate groups (Information Information Figure S5b). Except for compound **5**, the solvent molecules are all coordinated to Zn^{2+} from Zn clusters in other four MOFs, which indicate that the solvent plays a key role in the formation of different Zn clusters. The size and polarity of solvents have a great influence on different MOF architectures. With solvent as the only variable, we have successfully achieved solvent-controlled synthesis of MOFs.

More strikingly, compound **1**·DMSO can be employed as a precursor in various organic solvents for stepwise synthesis via SCSC transformation. Typically, as-synthesized **1**·DMSO was solvothermally treated with respective solvents in a Teflon reactor to accordingly afford organic-solvent-substituted single crystals, namely, **1**·DMF, **1**·DMA, **1**·EtOH (**1**·DMF has been reported by Cao group recently[12]), in which not only isolated solvents but also the terminally coordinated DMSO were replaced by new solvent molecules based on single-crystal structural determination and ^{1}H NMR studies (Figure 2 and Supporting Information Figures S7−9). The as-prepared MOFs were soaked in $CDCl_3$ solution for 24 h and then ^{1}H NMR spectrum of these filtrate were measured. The results have shown that **1**·DMSO, **1**·DMF, **1**·DMA, and **1**·EtOH only involve DMSO/EtOH, DMF, DMA, and EtOH, respectively, which demonstrate that solvent-exchange in these MOFs has been thoroughly realized during SCSC process. Interestingly, although the framework topologies are almost the same, these structures with different solvents are slightly different. The distances among central C and benzene ring and metal cluster centers change correspondingly (Supporting Information Figure S10 and Table S2). In contrast, the angle differences between the sides associated with central C to benzene ring centers in these structures are more pronounced attributed to the flexibility of the frameworks. Similarly, framework geometry in response to the size of the guest solvents in MOFs was reported recently.[19] Significantly, **1**·EtOH further transforms to **1**·H_2O upon exposure to air. The structure of **1**·H_2O crystallizes in a different space group of *P*4/*ncc* and involves one Zn atom, one H_2O and one L with a 1/4 occupancy factor in its asymmetric unit. Each oxygen in L coordinates to one Zn atom and two adjacent Zn atoms connected by one carboxylic group combine to the Zn_2 cluster in a paddle-wheel environment that coordinated by two H_2O molecules at axial positions and four carboxylate groups from four L ligands, thus to afford a 3D network with (4,8)-connected **scu** topology (Figure 2 and Supporting Information Figure S11). In comparison with **1**·DMSO, they have the similar framework topology, but different space groups and architectures from the same view direction (Supporting Information Figure S12). Notably, as displayed in Figure 2, except that **1**·DMSO and **1**·DMF can be synthesized from direct one-pot reaction, all other compounds should be obtained in a stepwise approach. Especially, we have succeeded in synthesis of **1**·H_2O only by a three-step route, but not successful either one or two steps. It is really difficult and unusual that the stepwise SCSC transformation of the three MOFs (**1**·DMSO, **1**·EtOH, and **1**·H_2O) involving significant crystallographic changes has been successfully realized.

The appropriate pore size (10−12 Å) and permanent porosity of **1**·DMSO demonstrated by N_2 sorption studies (BET surface area: 870 m^2/g) make it suitable as a host for

dx.doi.org/10.1021/ic202635a | *Inorg. Chem.* 2012, 51, 7484−7491

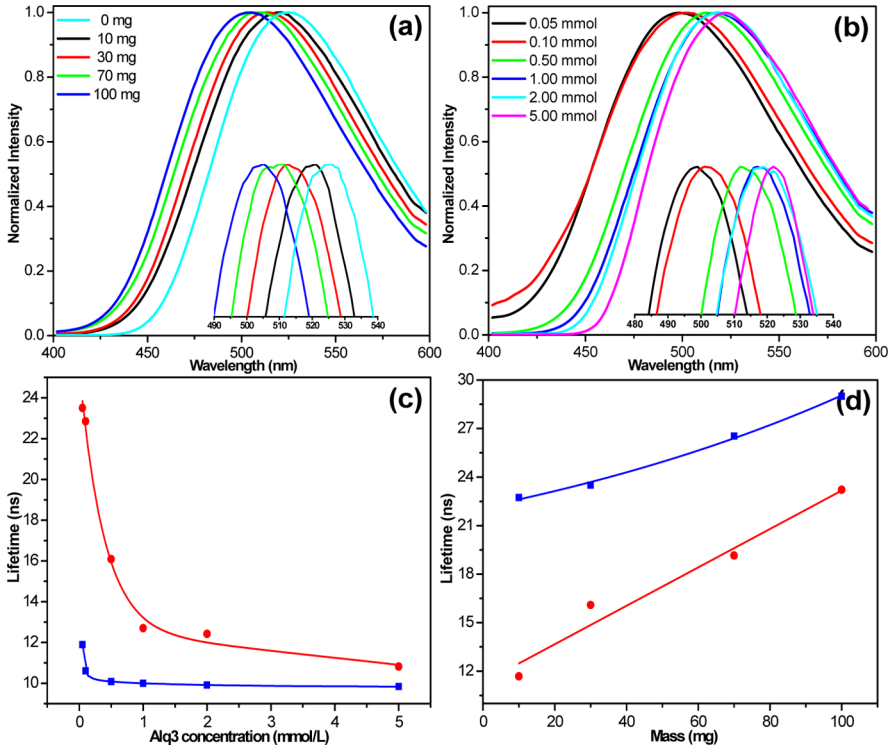

Figure 4. Fluorescence spectra of (a) 0.5 mmol/L Alq3 in DMF solutions (3 mL) with different amounts of **1**·DMSO, (b) Alq3 with various concentrations and 30 mg **1**·DMSO in DMF solutions (3 mL) under λ_{ex} = 360 nm. Insets: enlarged emission peaks. (c) Fluorescence lifetimes of Alq3 with different concentrations in DMF (3 mL) in the absence (blue) or presence (red) of 30 mg **1**·DMSO addition. (d) Fluorescence lifetimes of 0.05 mmol/L (blue) and 0.5 mmol/L (red) Alq3 in DMF (3 mL) with different amounts of **1**·DMSO addition. The curves in c and d are to guide the eye and not fit to the data. The excitation wavelength for all fluorescence lifetime measurements are 360 nm except for samples without **1**·DMSO addition.

encapsulating Alq3 molecules (the size of 8−9 Å). The crystalline **1**·DMSO was introduced into the 5.0 mmol/L Alq3 DMF solution. The colorless crystals gradually turn to yellow after 48 h (Supporting Information Figure S13). TGA curves (Supporting Information Figure S14a) and the Inductive Coupled Plasma (ICP) analysis (Supporting Information Table S3) results show that 15.8 wt % Alq3 was loaded in **1**·DMSO and each large cage in **1**·DMSO can accommodate about one Alq3 molecule (Supporting Information Figure S15). The pure Alq3 in DMF show its characteristic fluorescence emission at 525 nm. Upon introduction of **1**·DMSO, the peak shifts to lower wavelength along with the increasing MOF amount (Figure 4a). Similarly, in the presence of fixed MOF amount, Alq3 with less concentration gives larger blue shift (Figure 4b). More importantly, as displayed in Figure 4c, the excited-state lifetime of Alq3 chromophore in the Alq3@MOF composite is efficiently prolonged compare to the pure Alq3. In the solutions with the same Alq3 concentration, the fluorescence lifetime is nearly linear to MOF amount introduced in our examined range (Figure 4d). As compared to Alq3 in solution, the geometrical distortion of Alq3 at excited state becomes smaller upon absorption into MOF, which results in the blue shift of its emission spectrum, the decrease in nonradiative rate due to vibration and or rotation, and thus the increase in its lifetime.[20] The present study demonstrates the advantage of employing MOF as a host to modulate the luminescent properties of Alq3, which makes the Alq3@MOF hybrid composite a good candidate for improving the performance of Alq3-based opto-electronic devices.

Luminescent compounds are of great current interest because of their various applications in chemical sensors, photochemistry and electroluminescent display.[21] The luminescent property of zinc carboxylate compounds have been investigated.[22] The emission maximum for H_8L ligand is 436 nm (λ_{ex} = 371 nm) at ambient temperature. In comparison with the multicarboxylate ligand, the emission maxima of compounds **1**·DMSO and **2**−**5** have changed (Supporting Information Figure S21). The emission maxima for the compounds **1**·DMSO and **2**−**5** are 404, 446, 483, 421, and 463 nm (λ_{ex} = 328 nm for **1**·DMSO, λ_{ex} = 343 nm for **2**, λ_{ex} = 358 nm for **3**, λ_{ex} = 355 nm for **4**, and λ_{ex} = 362 nm for **5**), which exhibit the shift (32, 10, 47, 15, and 27 nm) with respect to the free H_8L ligand. The results may be attributed to a joint contribution of the intraligand transitions or charge transfer transitions between the coordinated ligands and the metal center.[23]

CONCLUSION

In summary, for the first time, we have systematically integrated solvent-controlled MOF architectures and SCSC transformation, as well as stepwise even multistep synthesis in one work. The Zn-L-based MOFs exhibit unusual structural diversity triggered by solvent only owing to the flexibility of ligand. The solvent-induced SCSC transformation involves not only solvent exchange but also the cleavage and formation of coordination bonds. Especially, the three-step SCSC transformation causes significant crystallographic change that cannot be realized by one- or two-step. Furthermore, we have first demonstrated that the MOF could be excellent host for chromophores such as

dx.doi.org/10.1021/ic202635a | Inorg. Chem. 2012, 51, 7484−7491

Alq3 for modulated luminescence and prolonged lifetime. Such encouraging results afford new opportunities for the rapidly growing MOF family in luminescent applications.

■ ASSOCIATED CONTENT

Supporting Information

Crystallographic data (CIF), PXRD, NMR spectra, TG curves of compounds, luminescence data, additional figures, and N_2 sorption isotherm. These material are available free of charge via the Internet at http://pubs.acs.org.

■ AUTHOR INFORMATION

Corresponding Author

*E-mail: q.xu@aist.go.jp.

Author Contributions

§Y.-Q.L. and H.-L.J. contributed equally to this work.

Notes

The authors declare no competing financial interest.

■ ACKNOWLEDGMENTS

We gratefully thank AIST and JSPS for financial support. Y.Q.L. thanks JSPS for a postdoctoral fellowship.

■ REFERENCES

(1) (a) Eddaoudi, M.; Kim, J.; Rosi, N.; Vodak, D.; Wachter, J.; O'Keeffe, M.; Yaghi, O. M. *Science* **2002**, *295*, 469. (b) Férey, G.; Mellot-Draznieks, C.; Serre, C.; Millange, F. *Acc. Chem. Res.* **2005**, *38*, 217. (c) Horike, S.; Shimomura, S.; Kitagawa, S. *Nat. Chem* **2009**, *1*, 695. (d) Corma, A.; García, H.; Llabrés i Xamena, F. X. *Chem. Rev.* **2010**, *110*, 4606. (e) Farha, O. K.; Hupp, J. T. *Acc. Chem. Res.* **2010**, *43*, 1166.

(2) (a) Seo, J. S.; Whang, D.; Lee, H.; Jun, S. I.; Oh, J.; Jeon, Y. J.; Kim, K. *Nature* **2000**, *404*, 982. (b) Pan, L.; Olson, D. H.; Ciemnolonski, L. R.; Heddy, R.; Li, J. *Angew. Chem., Int. Ed.* **2006**, *45*, 616. (c) Cheon, Y. E.; Suh, M. P. *Angew. Chem., Int. Ed.* **2009**, *48*, 2899. (d) Kitagawa, H. *Nat. Chem.* **2009**, *1*, 689. (e) Murray, L. J.; Dincă, M.; Long, J. R. *Chem. Soc. Rev.* **2009**, *38*, 1294. (f) Ma, S.; Zhou, H. C. *Chem. Commun.* **2010**, *46*, 44. (g) Jiang, H. L.; Xu, Q. *Chem. Commun.* **2011**, *47*, 3351. (h) Cui, Y.; Yue, Y.; Qian, G.; Chen, B. *Chem. Rev.* **2012**, *112*, 1126.

(3) (a) Lin, X.; Jia, J.; Zhao, X.; Thomas, K. M.; Blake, A. J.; Walker, G. S.; Champness, N. R.; Hubberstey, P.; Schröder, M. *Angew. Chem., Int. Ed.* **2006**, *45*, 7358. (b) Zhao, D.; Timmons, D. J.; Yuan, D.; Zhou, H.-C. *Acc. Chem. Res.* **2011**, *44*, 123.

(4) (a) Ma, L.; Lin, W. *J. Am. Chem. Soc.* **2008**, *130*, 13834. (b) Senkovska, I.; Kaskel, S. *Eur. J. Inorg. Chem.* **2006**, 4564. (c) Li, C. P.; Du, M. *Chem. Commun.* **2011**, *47*, 5958.

(5) (a) Kitagawa, S; Uemura, K. *Chem. Soc. Rev.* **2005**, *34*, 109. (b) Vittal, J. J. *Coord. Chem. Rev.* **2007**, *252*, 1781. (c) Wang, Z.; Cohen, S. M. *Chem. Soc. Rev.* **2009**, *38*, 1315. (d) Leong, W. L.; Vittal, J. J. *Chem. Rev.* **2011**, *111*, 688. (e) Kitagawa, S.; Kitaura, R.; Noro, S.-i. *Angew. Chem., Int. Ed.* **2004**, *43*, 2334.

(6) (a) Wu, C. D.; Lin, W. *Angew. Chem., Int. Ed.* **2005**, *44*, 1958. (b) Maji, T. K.; Mostafa, G.; Matsuda, R.; Kitagawa, S. *J. Am. Chem. Soc.* **2005**, *127*, 17152. (c) Zhang, J.-P.; Lin, Y.-Y.; Zhang, W.-X.; Chen, X.-M. *J. Am. Chem. Soc.* **2005**, *127*, 14162. (d) Jiang, H. L.; Tatsu, Y.; Lu, Z. H.; Xu, Q. *J. Am. Chem. Soc.* **2010**, *132*, 5586. (e) Liu, Q.-K.; Ma, J.-P.; Dong, Y.-B. *J. Am. Chem. Soc.* **2010**, *132*, 7005. (f) Chen, M.-S.; Chen, M.; Takamizawa, S.; Okamura, T.; Fan, J.; Sun, W.-Y. *Chem. Commun.* **2011**, *47*, 3787.

(7) (a) Das, M. C.; Bharadwaj, P. K. *J. Am. Chem. Soc.* **2009**, *131*, 10942. (b) Bernini, M. C.; Gándara, F..; Iglesias, M.; Snejko, N.; Gutiérrez-Puebla, E.; Brusau, E. V.; Narda, G. E.; Monge, M. Á. *Chem.—Eur. J.* **2009**, *15*, 4896. (c) Zhuang, C.-F.; Zhang, J.; Wang, Q.; Chu, Z.-H.; Fenske, D.; Su, C.-Y. *Chem.—Eur. J.* **2009**, *15*, 7578. (d) Park, H. J.; Cheon, Y. E.; Suh, M. P. *Chem.—Eur. J.* **2010**, *16*, 11662. (e) Aijaz, A.; Lama, P.; Bharadwaj, P. K. *Inorg. Chem.* **2010**, *49*, 5883.

(8) Cui, Y.; Yue, Y.; Qian, G.; Chen, B. *Chem. Rev.* **2012**, *112*, 1126.

(9) (a) Suh, M.; Cheon, Y.; Lee, E. *Coord. Chem. Rev.* **2008**, *252*, 1007. (b) Rocha, J.; Carlos, L. D.; Paz, F. A. A.; Ananias, D. *Chem. Soc. Rev.* **2011**, *40*, 926. (c) Allendorf, M. D.; Bauer, C. A.; Bhakta, R. K.; Houk, R. J. T. *Chem. Soc. Rev.* **2009**, *38*, 1330. (d) Chen, B.; Xiang, S.; Qian, G. *Acc. Chem. Res.* **2010**, *43*, 1115. (e) Shekhah, O.; Liu, J.; Fischer, R. A.; Wöll, C. *Chem. Soc. Rev.* **2011**, *40*, 1081. (f) Férey, G. *Chem. Soc. Rev.* **2008**, *37*, 191. (g) Kuppler, R. J.; Timmons, D. J.; Fang, Q.-R.; Li, J.-R.; Makal, T. A.; Young, M. D.; Yuan, D.; Zhao, D.; Zhuang, W.; Zhou, H.-C. *Coord. Chem. Rev.* **2009**, *253*, 3042.

(10) (a) Tang, C. W.; Van Slyke, S. A. *Appl. Phys. Lett.* **1987**, *51*, 913. (b) Kido, J.; Kimura, M.; Nagai, K. *Science* **1995**, *267*, 1332. (c) Shen, Z. L.; Burrows, P. E.; Bulovic, V.; Forrest, S. R.; Thompson, M. E. *Science* **1997**, *276*, 2009. (d) Aziz, H.; Popovic, Z. D.; Hu, N. X.; Hor, A. M.; Xu, G. *Science* **1999**, *283*, 1900. (e) Chen, W.; Peng, Q.; Li, Y. D. *Adv. Mater.* **2008**, *20*, 2747.

(11) (a) Nguyen, T. Q.; Wu, J.; Doan, V.; Schwartz, B. J.; Tolbert, S. H. *Science* **2000**, *288*, 652. (b) Zhang, X.; Shi, S.; Liu, Q.; Zhou, J.; Ye, J.; Yu, C. *Chem. Commun.* **2011**, *47*, 6359.

(12) Lin, Z.-J.; Liu, T.-F.; Zhao, X.-L.; Lü, J.; Cao, R. *Cryst. Growth Des.* **2011**, *11*, 4284.

(13) Zhuang, W.; Yuan, D.; Liu, D.; Zhong, C.; Li, J.-R.; Zhou, H.-C. *Chem. Mater.* **2012**, *24*, 18.

(14) (a) Sheldrick, G. M. *SHELXS-97, Programs for X-ray Crystal Structure Solution*; University of Göttingen: Göttingen, Germany, 1997. (b) Sheldrick, G. M. *SHELXL-97, Programs for X-ray Crystal Structure Refinement*; University of Göttingen: Göttingen, Germany, 1997. (c) Farrugia, L. J. *WINGX, A Windows Program for Crystal Structure Analysis*; University of Glasgow: Glasgow, U.K., 1988. (d) Spek, A. L. *PLATON*, A multipurpose crystallographic tool, Utrecht. University, Netherlands, 2001.

(15) (a) Dolomanov, O. V. *OLEX*, http://www.ccp14.ac.uk/ccp/web-mirrors/lcells/index.htm. (b) Dolomanov, O. V.; Blake, A. J.; Champness, N. R.; Schroder, M. *J. Appl. Crystallogr.* **2003**, *36*, 1283.

(16) (a) Batten, S. R.; Robson, R. *Angew. Chem., Int. Ed.* **1998**, *37*, 1460. (b) Natarajan, R.; Savitha, G.; Dominiak, P.; Wozniak, K.; Moorthy, J. N. *Angew. Chem., Int. Ed.* **2005**, *44*, 2115. (c) Hill, R. J.; Long, D. L.; Champness, N. R.; Hubberstey, P.; Schröder, M. *Acc. Chem. Res.* **2005**, *38*, 335. (d) Chen, B.; Ockwig, N. W.; Fronczek, F. R.; Contreras, D. S.; Yaghi, O. M. *Inorg. Chem.* **2005**, *44*, 181. (e) Xue, M.; Zhu, G.; Li, Y.; Zhao, X.; Jin, Z.; Kang, E.; Qiu, S. *Cryst. Growth Des.* **2008**, *8*, 2478. (f) *Coordination Polymers: Design, Analysis and Application*; Batten, S. R., Neville, S. M., Turner, D. R., Ed.; Royal Society of Chemistry: Cambridge, U.K., 2009.

(17) (a) Chun, H.; Kim, D.; Dybtsev, D. N.; Kim, K. *Angew. Chem., Int. Ed.* **2004**, *43*, 971. (b) Zou, R.-Q.; Zhong, R.-Q.; Du, M.; Kiyobayashi, T.; Xu, Q. *Chem. Commun.* **2007**, 2467. (c) Zhai, Q.-G.; Lu, C.-Z.; Wu, X.-Y.; Batten, S. R. *Cryst. Growth Des.* **2007**, *7*, 2332. (d) Lan, Y. Q.; Li, S. L.; Li, Y. G.; Su, Z. M.; Shao, K. Z.; Wang, X. L. *CrystEngComm* **2008**, *10*, 1129. (e) Ma, L. Q.; Mihalcik, D. J.; Lin, W. B. *J. Am. Chem. Soc.* **2009**, *131*, 4610. (f) Jiang, H.-L.; Lin, Q.-P.; Akita, T.; Liu, B.; Ohashi, H.; Oji, H.; Honma, T.; Takei, T.; Haruta, M.; Xu, Q. *Chem.—Eur. J.* **2011**, *17*, 78.

(18) (a) Wu, J.-Y.; Yang, S.-L.; Luo, T.-T.; Liu, Y.-H.; Cheng, Y.-W.; Chen, Y.-F.; Wen, Y.-S.; Lin, L.-G.; Lu, K.-L. *Chem.—Eur. J.* **2008**, *14*, 7136. (b) Liu, H.-S.; Lan, Y.-Q.; Li, S.-L. *Cryst. Growth Des.* **2010**, *10*, 5221.

(19) Nelson, A. P.; Parrish, D. A.; Cambrea, L. R.; Baldwin, L. C.; Trivedi, N. J.; Mulfort, K. L.; Farha, O. K.; Hupp, J. T. *Cryst. Growth Des.* **2009**, *9*, 4588.

(20) *Principles of Molecular Photochemistry: An Introduction*; Turro, N. J., Scaiano, J. C., Ramamurthy, V., Eds.; University Science Books: Sausalito, CA, 2008.

(21) (a) Wu, Q.; Esteghamatian, M.; Hu, N.-X.; Popovic, Z.; Enright, G.; Tao, Y.; D'Iorio, M.; Wang, S. *Chem. Mater.* **2000**, *12*, 79. (b) McGarrah, J. E.; Kim, Y.-J.; Hissler, M.; Eisenberg, R. *Inorg. Chem.*

2001, *40*, 4510. (c) Santis, G. D.; Fabbrizzi, L.; Licchelli, M.; Poggi, A.; Taglietti, A. *Angew. Chem., Int. Ed.* **1996**, *35*, 202.
(22) Zheng, S.-L.; Yang, J.-H.; Yu, X.-L.; Chen, X.- M.; Wong, W.-T. *Inorg. Chem.* **2004**, *43*, 830.
(23) (a) Li, S.-L.; Lan, Y.-Q.; Ma, J.-F.; Yang, J.; Wei, G.-H.; Zhang, L.-P.; Su, Z.-M. *Cryst. Growth Des.* **2008**, *8*, 675. (b) Li, S.-L.; Lan, Y.-Q.; Ma, J.-F.; Fu, Y.-M.; Yang, J.; Ping, G.-J.; Liu, J.; Su, Z.-M. *Cryst. Growth Des.* **2008**, *8*, 1610.